



Cite this: *Sustainable Energy Fuels*, 2023, 7, 4898

Life-cycle assessment of renewable fuel production via hydrothermal liquefaction of manure in Germany†

Leonard Moser, Benjamin W. Portner, Christina Penke, Kathrin Ebner and Valentin Batteiger

Hydrothermal liquefaction (HTL) is a promising option for transforming wet feedstock into liquid fuels. In this work, the Global Warming Potentials (GWP) of HTL fuels obtained from manure have been analyzed for different process configurations using life-cycle assessment (LCA). The GWP of the baseline case amounts to 1.18 kg CO₂-eq. per kg_{fuel mix}, which equals to an emission reduction of about 70% compared to conventional jet fuel. Key emission drivers are H₂ production via steam methane reforming (SMR) and process heat provision from natural gas. Improvements are observed when the H₂ demand is covered by reforming of internally produced biogas or water electrolysis. The latter option is highly sensitive to the carbon intensity (CI) of the electricity input. As a consequence of different CIs, the best performing HTL process configuration strongly depends on the respective local electricity supply. Moreover, the potential emission savings from reduced manure storage durations are analyzed and quantified as -0.38 kg CO₂-eq. per kg manure. Integration into a consequential LCA approach leads to carbon negative fuel production via the HTL pathway in most of the investigated scenarios.

Received 17th May 2023
Accepted 27th July 2023

DOI: 10.1039/d3se00646h
rsc.li/sustainable-energy

Introduction

The European Union has pledged to achieve climate neutrality by 2050, delivering on its commitments under the Paris Agreement.¹ Achieving this target requires rethinking established practices, especially in economic sectors that contribute significantly to the current greenhouse gas (GHG) emission budget. So far, measures to reduce overall GHG emissions in agriculture and transportation have not been effective.^{2,3}

The transportation sector accounts for about one third of the EU GHG emission budget.^{4,5} GHG emissions from transportation are predominantly linked to fuel use. It is likely that battery-electric vehicles and, to a lesser extent, H₂ and fuel cells, will play a dominant role in the decarbonization of transportation. However, specific transportation sectors, most notably aviation, will continue to rely on liquid hydrocarbon fuels for decades.⁶ Advanced biofuels from residues and wastes present promising options that can contribute to the future supply of sustainable liquid hydrocarbon fuels.

To this end, the utilization of manure could enlarge the raw material pool for advanced biofuel production. At the same time, manure conversion could be linked with an emission reduction in the agricultural sector. In 2021, the agricultural

sector accounted for about 8% of Germany's total GHG emissions.³ Farm fertilizer, which is dominated by manure (85%) contributes about 16% of all agricultural GHG emissions.^{3,7,8} GHG emissions from manure management mainly stem from CH₄ and N₂O emissions, which are almost exclusively attributed to manure storage.^{9,10} Normalizing these emissions by the amount of manure produced in Germany results in about 0.6 kg CO₂-eq. per kg manure.¹⁰⁻¹² A key variable in reducing these emissions is the duration of storage. Continuous use of manure as a feedstock for fuel production can reduce storage durations and presents a lever for significant emission avoidance.

Hydrothermal liquefaction (HTL) has emerged as a promising option for the conversion of a broad range of organic feedstock into an intermediate biocrude, which subsequently can be upgraded to liquid hydrocarbon fuels via hydro-treating.¹³ HTL is in particular suitable for wet feedstock, such as sewage sludge and manures, the conversion of animal excretions via HTL has therefore been studied for more than a decade.¹⁴⁻²⁰ Within a catchment area of 10 km, the highest theoretical feedstock potentials in Europe have been found in the range of 150 kt dry matter (DM) per year for cattle manure.²¹ Therefore, the utilization of HTL for manure conversion unlocks significant potential for liquid transportation fuel production.

This paper aims to provide a detailed LCA of the HTL fuel production pathway with manure as feedstock, focusing on a future commercial plant in Germany. Furthermore, different process configurations of the HTL pathway are

Bauhaus Luftfahrt e.V., 82024 Taufkirchen, Germany. E-mail: leonard.moser@bauhaus-luftfahrt.net

† Electronic supplementary information (ESI) available. See DOI: <https://doi.org/10.1039/d3se00646h>



studied, providing valuable insights for the field of LCA studies on HTL fuel production. In particular, utilization of internally produced biogas for H₂ production *via* SMR as well as utilization of electricity for process heat and H₂ generation are compared to the baseline case scenario, in which heat and H₂ are produced from natural gas (NG).

Methodology

The methodology section of this manuscript comprises three major parts. First, general methodological details on life-cycle assessment (LCA) are given. Next, the HTL fuel production model is described. The third part deals with the description of the manure reference process.

Life-cycle assessment

LCA is a methodology to conduct environmental impact assessments standardized in ISO 14040 and ISO 14044.^{22,23} In this work, we performed LCA with the Brightway2 software, using the Activity Browser as a graphical user interface.²⁴ Typically, an LCA includes four stages:

- Goal and scope definition.
- Inventory analysis (LCI).
- Impact analysis (LCIA).
- Interpretation.

Goal and scope

This assessment has three goals: (1) quantify the climate change impact (GWP100) of fuel production from hydro-thermal liquefaction. (2) Perform a scenario analysis on parameters that strongly affect the climate change impact (GWP100) of HTL fuel production. (3) Analyze the potential GHG emission savings from an alternative manure management practice in Germany. This study intends to create awareness among sustainability and renewable fuel experts about the environmental impact associated with current manure management practice and the potential benefits of effective repurposing. Furthermore, this work aims at advancing knowledge on the HTL fuel production pathway, which can help to decarbonize transportation and thus mitigate climate change. For comparability and verification purposes, all data will be disclosed and are available in the ESI.† Details on the modeling assumptions are discussed below. For the baseline (BL) case, it is assumed that manure comes free of upstream burdens (cut-off approach). Manure collection and transport present the starting point in this model. In addition to the cut-off approach, an alternative consequential approach is discussed. Fuel combustion is implicitly modelled as the re-release of biogenic carbon into the atmosphere.

Inventory analysis (LCI)

The LCI comprises material and energy inputs/outputs for the entire life cycle of HTL fuel production, starting from manure collection and transport over conversion to fuel transport and subsequent fuel use. Background activities are modeled using

the Ecoinvent 3.7.1 database, APOS system model.²⁵ Foreground activities are modeled in Brightway2 and made available in the ESI.†

Impact analysis (LCIA)

The herein performed impact assessment is focused on the category of climate change. Characterization factors from the “ReCiPe 2016, 1.1 (20180117), Midpoint, Global Warming, 100 year timescale, Hierarchist” method are used.²⁶ Characterization factors for biogenic CH₄ and N₂O are 34 and 298 kg CO₂-eq. per kg gas, respectively.²⁶⁻²⁸

All results are based on the functional unit of 1 kg of hydro-treated and distilled HTL product. This fuel mix consists of the following liquid product fractions: naphtha, jet fuel, diesel and heavy fuel oil. The choice of 1 kg_{fuel mix} as functional unit corresponds to the product output of a simple HTL refinery concept that only involves the necessary hydrotreatment and fractionation. As a consequence, a specific composition of the feedstock directly translates into a specific composition of the fuel product. Table 1 lists the product fractions of the different fuel types for manure 1 and manure 2, which result from the Aspen Plus® model used as basis for the study.²⁹ Details on the Aspen Plus® model will be discussed later. In particular, we do not consider additional refining steps that can tailor the composition of the fuel mix towards a specific target product at the cost of other liquid hydrocarbon fuel fractions. This approach ensures a high generality of our LCIA results. The fractionated mix of upgraded HTL fuel corresponds to the fractionated output of a conventional refinery. In the section “Results and Discussion” we choose the GWP of conventional jet fuel as a specific comparator (see Fig. 4), but the results may as well be compared to naphtha for the renewable chemistry, diesel or heavy fuel oil for the marine sector.

Interpretation

The LCIA results are discussed and interpreted in the “Results and Discussion” section. This includes interpretation and conclusions from the baseline case as well as the scenario analysis, including scenarios resulting from a cut-off LCA approach only looking at the fuel production, as well as consequential LCA scenarios, including the impact of upstream manure supply. Based on the baseline case, several key parameters, such as the heat and hydrogen supply (different process configurations), the carbon intensity (CI) of the electricity input and the chemical composition of the manure feedstock were identified and varied (see Fig. 4 and 5). Limitations and issues related to data uncertainty are also

Table 1 Fuel fractions and their respective yield from the HTL process for manure samples 1 and 2. Boiling ranges are used based on ref. 13

Fraction	Manure 1	Manure 2
Naphtha (27–193 °C)	19.8	14.9
Jet fuel (194–271 °C)	31.1	28.4
Diesel (272–425 °C)	44.0	51.6
Heavy fuel oil (>425 °C)	5.1	5.1



discussed. Furthermore, recommendations for future work in this field are given.

Baseline process configuration and modelling

The baseline process configuration is based on a concept for HTL fuel production that was investigated in the EU-H2020 project HyFlexFuel. The fuel production system includes the following process steps:³⁰

- Manure collection and transport.
- Manure pretreatment.
- Hydrothermal liquefaction (HTL).
- Treatment of the HTL aqueous phase (AP).
- Nutrient recovery (NR).
- Hydrotreatment (HT).
- Treatment of the HT offgas.
- Process heat production.
- H₂ production.
- Fuel transport.

Modelling of the HTL, HT, catalytic hydrothermal gasification (cHTG) and NR process steps has been performed in Aspen Plus®. The model and results for the conversion of other feedstock (Spirulina, sewage sludge and wheat straw) have been described and published before.^{29,31} The feedstock biomass is modelled by more than 50 chemical compounds representing the hydrolysis products of the main biochemical groups as well as the ash components. This allows modelling of various biomass feedstock. The three major process steps (HTL, HT, cHTG) are modelled with an RStoic reactor, including more than 270 reactions each. To our knowledge, this is the only Aspen Plus® model investigating the extremely complex HTL reaction network in such depth. Nevertheless, fractional conversion factors need to be adapted such that the resulting streams match experimental results. The main results that can be deduced from the model are mass and energy balances, including biogas production from cHTG, biocrude and upgraded biocrude yield, H₂ consumption in the HT unit and fuel fractions after distillation. Furthermore, data on individual streams, such as gas compositions, elemental analysis of all streams, boiling point distributions, chemical compositions, molecular mass distributions and densities of biocrude and upgraded biocrude streams can be obtained from the modelling. Details on these results are given in Tables S2–S5 and Fig. S1 in the ESI.†

In addition to the in-depth representation of the main chemical conversion process, further assumptions are required for an LCA of the entire process chain. In the baseline case, modelling of the entire process chain starts with manure collection and transport. Manure is collected at the farm and transported to the HTL plant by truck over a distance of 50 km. It is assumed that manure has an average dry matter (DM) content of 10 wt%.³² In a pre-treatment step, the DM content is increased to 20 wt% using a centrifuge. This ensures the thermal efficiency of the HTL process while still maintaining pumpability of the feed slurry. The feed slurry is pressurized to 220 bar and then preheated by heat exchange with the HTL product streams. In terms of energy recovery, it was assumed that 80% of the heat demand of each process can be recovered from the hot product side. Subsequently,

the reaction temperature of 350 °C is reached using a boiler. After conversion, the HTL product mixture is cooled down to 80 °C to achieve separation of the four product phases: biocrude, HTL aqueous phase (AP), HTL solids and HTL gas phase. The main product, a biocrude, is transferred to the hydrotreating unit, where it is reacted with an excess amount of H₂ at 400 °C temperature and 70 bar pressure to yield a mixture of transportation fuels. H₂ is produced *via* steam methane reforming (SMR) of natural gas. SMR is modelled based on literature data and on a stoichiometric calculation with direct fossil CO₂-emissions.³³ The carbon intensity of the electricity input is given by the German grid mix in 2019.³⁴ The HT model accounts for the energy demand of catalytic hydrotreating and vacuum distillation. Subsequent transport of the HT product fuel mix to the airport/gas station is modelled by truck transport over a distance of 200 km.

Apart from the main product, the sustainability and economic feasibility of the pathway depend on the effective valorisation of the HTL and HT side streams. HT produces an off-gas, which consists primarily of excess H₂. Two consecutive pressure swing adsorption (PSA) units recover this H₂ and cycle it back to the HT unit. The remaining HT off-gas is rich in gaseous hydrocarbons and used together with the HTL off-gas for internal heat production. The HTL aqueous phase (AP) contains up to 50% of the manure carbon, which is recovered as biogas *via* catalytic hydrothermal gasification (cHTG). The AP is passed through a salt separator to remove salts and metals, which inhibit the ruthenium based cHTG catalyst. The AP is then pressurized to 280 bar and heated to 400 °C before entering the cHTG reactor. In the model, 90% of the organic content in the AP is converted into biogas (50 vol% CH₄, 35 vol% CO₂, 15 vol% H₂O, NH₃ and others). Brine from the salt separator as well as HTL solids, serve as an input for NR. Since phosphorous is defined as scarce material by the European Commission, NR may be mandatory in the near future.³⁵ NR consists of three steps. In a first leaching step, the HTL solids are mixed with a 1 M sulphuric acid solution dissolving 50% of the solids. Unsolvable remnants are treated as solid waste. In a second step, the dissolved solids are mixed with the brine phase from the cHTG unit and a magnesium source, *e.g.* magnesium sulphate. Finally, the pH value of the solution is shifted to alkaline (pH = 9), to initiate the precipitation of struvite, a solid fertilizer. Due to a lack of quantitative data, it was assumed that fertilizers (manure, inorganic fertilizer, struvite) and the digestate of anaerobic digestion (manure reference process) have the same bioavailability and subsequent fertilizing effect associated with an equal amount of nutrient (nitrogen or phosphorous).

Although no specific data is available at the time of writing, experimental results within the HyFlexFuel project allowed to distinguish at least two different grades of pollution.³⁰ The process water after cHTG is significantly less polluted than the process water from NR.

Fuel production scenarios

Scenario analysis of the HTL fuel production pathway is performed on the following parameters:



- H₂ provision (SMR *vs.* alkaline water electrolysis (AEL)).
- Heat provision (natural gas *vs.* product gas *vs.* electrical heating).
- GHG intensity of the electricity input.
- Manure composition.
- Manure reference process (cut-off *vs.* consequential modeling).

Parameters 1 to 4, which are varied in the cut-off approach scenarios, are described in this section. The manure reference process, which is the essential part of the consequential modelling, will be described in the section "Modelling of manure reference process".

The variation of heat and H₂ supply leads to five different process configurations. Besides the Baseline (BL) process configuration, Fig. 1 shows two other process configurations (SMR-BG and AEL-BG), which differ in terms of H₂ provision. AEL was chosen because it is well established and state-of-the-art. The AEL unit consumes 56.5 kW h of power per kg H₂ at an outlet pressure of 33 bar.^{36,37} It is assumed that the unit consists of multiple 1 MW stacks at a yearly operation time of 8300 hours. The inventory includes the production of the electrolyzer unit and the Balance of Plant (BOP), considering material inputs for cell and stack construction as well as water, electrolyte, electricity and other operational inputs for H₂ production.^{36,37} BOP includes inputs for electronic equipment as well as pumps and tanks (full description in the ESI†). In addition, the impact of the heat source is investigated in two further configurations, which employ electrical resistance heating. The use of internally produced biogas (BG) differs significantly in the different process configurations. In the BL-scenarios, all of the internally produced BG is used to substitute heat on the market for heat, while in the SMR-NG/EL-scenarios internally produced biogas is firstly used for H₂ supply *via* SMR. CO₂-emissions from SMR of internally produced biogas (SMR scenarios) are biogenic and carry no climate impact.‡ Excess biogas is subsequently used for internal heat production. In the AEL-BG/EL-scenarios, biogas is firstly used for internal heat production, while excess biogas is used to substitute heat on the market for heat.

Three different carbon intensities (CIs) for the electricity input are chosen to represent the German grid mix (GGM) from 2019 (baseline case), as well as two future grid mixes with an increased share of renewable electricity. Table 2 gives an overview of the three chosen CIs. From a chemical perspective, manure is a very diverse feedstock. Table S1† lists a number of proximate analyses of manures, showing their diversity. Differences arise from factors such as animal species, diet, manure storage conditions and duration. For the scenario analysis, two representative manure samples are compared.³⁸ The ultimate and proximate analyses are listed in Table 3. Differences in manure compositions have a variety of impacts on the final product. Fuel yield is influenced by feedstock ash content while the fuel mix composition (fuel fractions) and fuel properties (biochemical composition) are influenced by different proximate feedstock composition. In

summary, five different process configurations, three different CIs of the electricity input and two manure samples yield 30 different HTL fuel production scenarios discussed in the cut-off approach. For each process configuration, an exemplary scenario is defined in Table 4.

Modelling of an alternative manure management process

Manure is a side product of agricultural livestock breeding, the main products being milk and meat. As a consequence, increased manure demand does not automatically trigger additional manure production. Instead, manure consumption by new market actors (*e.g.* HTL operators) will reduce the availability of manure for other uses (fertilizer use, biogas production). The manure reference model accounts for the avoided burdens as well as foregone benefits of these current uses. Manure management involves two stages: (1) collection and storage and (2) use phase. Fig. 2 schematically depicts current practices.

Modelling of manure use

As mentioned above, CH₄ and N₂O emissions cause the largest part of the climate impact of manure management. It has been shown that GHG emissions from manure storage generally exceed GHG emissions from the use phase by up to three orders of magnitude.¹⁰ Current use of manure is modelled as fertilizer use for 67% of manure, while 33% is used for biogas production *via* anaerobic digestion. Substitution of the current manure practice leads to two changes in the emission balance:

- Avoided burdens due to the fact that emissions from the current uses are no longer emitted.
- Foregone benefits due to the fact that the products of the current uses have to be substituted by other production pathways.

Avoided burdens are generated by avoiding emissions from manure as fertilizer and from using manure as substrate for anaerobic digestion, since manure is used as feedstock for HTL. However, the products of these processes, namely energy in the form of heat and electricity from "biogas" as well as fertilizer in the form of manure have to be substituted by conventional products. In the case of fertilizer, this means that emissions resulting from conventional N and P fertilizer production need to be accounted for, while in the case of anaerobic digestion (AD), emissions from conventional heat and electricity production are considered. Electricity and heat production in the foreground system are adapted according to the respective HTL fuel production scenario from the cut-off approach.

Modelling of German manure mix

The German manure mix has been estimated based on livestock data and volatile solid excretions rates.^{10,12} It is dominated by cattle (85%) and swine (15%).

‡ It was decided to model the direct CO₂-emissions from SMR as fossil emissions and balance these emissions in the cHTG process step to emphasize the importance of the HTL AP for the environmental viability of the HTL process.



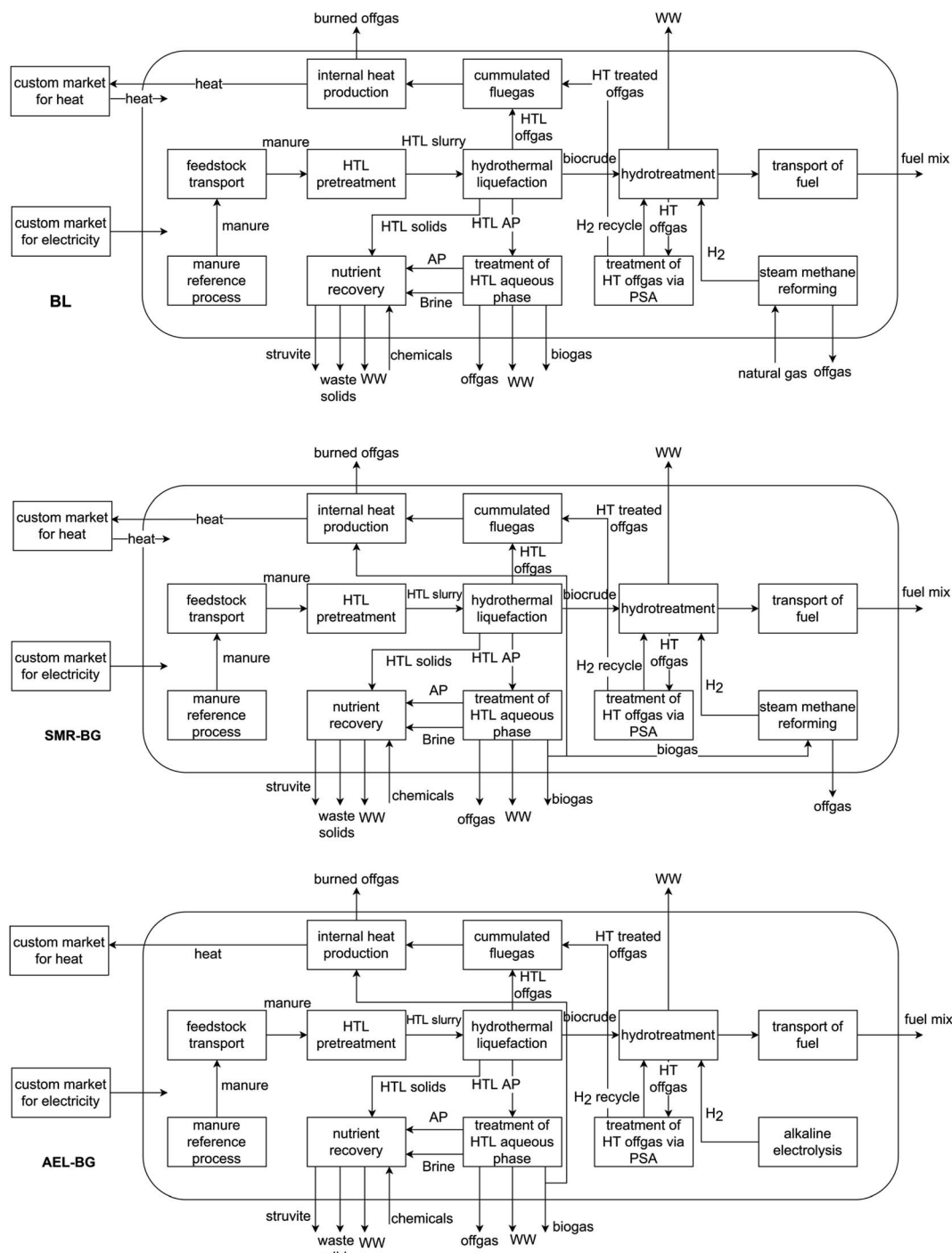


Fig. 1 Relevant process configurations investigated in this work. The main differences between the process configurations are: BL: H₂ production *via* steam methane reforming with natural gas, SMR-BG: H₂ production *via* steam methane reforming with internally produced biogas, AEL-BG: H₂ production *via* water electrolysis using electricity. HT: hydrotreatment; PSA: pressure swing adsorption; WW: wastewater.

Modelling of manure storage

Estimated emission data for manure management in Germany have been found in the FAOSTAT database.¹¹ Due to a lack of publicly available data on manure storage systems, we were not able to reproduce the value from the FAOSTAT database. In an effort to represent the range of possibilities, we differentiate the following two extreme cases: storage in uncovered anaerobic

lagoons (worst case) and storage in dry lots (best case). For both cases, literature values for emission factors from ref. 10 have been used to calculate the GHG emissions, assuming a storage time of six months (details in the SI).

GHG emissions from manure storage are time and temperature dependent. Therefore, a model that simulates the emissions of storage on a daily basis, by applying time and



Table 2 GHG intensities of different electricity production technologies^{34,39,40}

Electricity input	CI [g CO ₂ -eq. kW ⁻¹ h ⁻¹]
CI1	20
CI2	80
GGM	410

Table 3 Ultimate and proximate analyses of the two selected manures as used in the Aspen Plus® model based on ref. 38^a

Ultimate analysis						
Manure	C	H	N	O	S	Ash
1	49.3	6.9	2.9	40.2	0.7	38.6
2	53.1	7.3	5.3	33.7	0.5	17.0

Proximate analysis					
Manure	Lip	Car	Pro	Lig	Ext
1	2.9	46.8	7.4	4.1	0.8
2	8.6	48.4	20.5	5.3	0.8

^a Lip: lipids, Car: carbohydrates, Pro: proteins, Lig: lignin, Ext: extractives. All values are given in wt%.

temperature dependent emission profiles, is created. In this way, the estimated value from the FAOSTAT database can be disaggregated and emission savings due to a reduced storage duration can be quantified.^{10,41–43}

Based on the yearly seed times, different cases can be differentiated. In Germany, there are two seed times, leading to two fertilizer applications per year and therefore two manure storage periods between four and eight months. A significant temperature dependency of GHG emissions from manure storage can be observed, and GHG emissions during cold temperatures are <7% of GHG emissions during warmer periods.^{41–43} Therefore, only summer storage periods are considered in this work. Based on hourly temperature data for Germany, monthly average temperatures were calculated as arithmetic mean and used to create the emission profile for Germany (see Fig. S3†).⁴⁴ As already described,

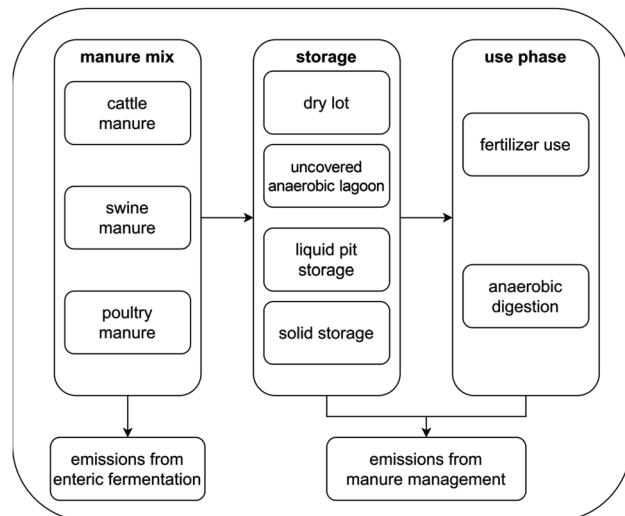


Fig. 2 Depiction of the current manure management practice.

GHG emissions from manure storage are composed of CH₄ and N₂O emissions. For CH₄ emissions, a threshold temperature of 13.93 °C was found,⁴¹ leading to cumulative emissions that are about 14 times higher than below the threshold temperature. For N₂O emissions there is a similarly strong temperature dependency.^{42,43} Since no particular threshold temperature is stated in the literature for N₂O emissions, the CH₄ value was used.

It is assumed that manure is collected once every day and that adding new manure does not affect the emissions of the already stored manure, *e.g.* through coverage or other mechanisms. For each month of storage, 28 days of storage and therefore 28 heaps of manure are assumed. Each heap of manure starts to emit CH₄ and N₂O one day later than the heap before. Depending on the temperature of the investigated month, we distinguish between a cold and a warm individual emission profile for both types of emissions (*cf.* Fig. S2†). The threshold temperature of 13.93 °C was used to decide, which individual emission profile was used each month to establish the cumulative emission profile. Adding up all individual emission profiles for each heap (or day) over a whole storage cycle creates a country specific cumulative emission profile. Assuming a shorter storage period, only a fraction of the emissions is released. Most importantly, subtracting the emissions for a shorter storage time from the estimated emissions give

Table 4 Abbreviations of different scenarios discussed in this paper. The first letters describe the used process configuration. It should be noted that all scenarios, which have the same process configuration (H2 and heat from NG) as the baseline case, are abbreviated with BL. The second part of the abbreviations describes the used market for heat (neglected in the baseline scenarios, since there is only one option (NG) in those scenarios). The third part describes the used electricity input while the fourth part shows the used manure sample. CHP: combined heat and power

Abbreviation	H ₂ provision	Heat provision	Electricity input	Manure
Baseline (BL-GGM-M1)	SMR of natural gas	Natural gas CHP	GGM	Manure 1
SMR-NG-CI1-M2	SMR of internal biogas	Natural gas CHP	CI1	Manure 2
AEL-NG-CI2-M2	Water electrolysis	Natural gas CHP	CI2	Manure 2
SMR-EL-CI1-M1	SMR of internal biogas	Electrical resistance heating	CI1	Manure 1
AEL-EL-CI2-M2	Water electrolysis	Electrical resistance heating	CI2	Manure 2



the emissions savings by the timely usage of manure in the HTL plant (*cf.* Fig. S3†).

Results and discussion

LCA of HTL fuel production pathway – cut-off approach

Baseline case. Fig. 3 shows the LCA Sankey diagram of the baseline scenario (BL-GGM-M1). The individual contributions are given relative to the total GWP100 score of 1.18 kg CO₂-eq. per kg_{fuel mix}. Red streams indicate an environmental burden, while green streams depict avoided emissions. Red boxes indicate a process step with net-emissions, while green boxes display process steps with a net-avoidance of emissions. It becomes evident that H₂ supply *via* SMR of natural gas (48%) has the highest impact in the BL scenario, followed by heat demand of the HTL unit (30%) and feedstock collection and transport (23%). Electricity for the HTL and cHTG unit also contributes significantly with 12% and 11%, respectively.

Wastewater treatment has an impact of 4%. Slightly polluted wastewaters fall below the threshold impact of 1% and are not shown. Major emission savings are generated by the substitution of heat from natural gas with internal heat production (−25%) from HT (−15%) and HTL (−8%) off-gases as well as from cHTG (−36%). They are indicated by the green process heat streams. Red process heat streams display that external input of process heat *via* natural gas is needed for the respective process. In the HTL BL-scenario (BL-GGM-M1), 46% of the total emissions trace back to a total of 9.1 MJ of external heat demand.

In conventional jet fuel is chosen as a comparator, while the GWP100 values in this study refer to a fractionated fuel mix as functional unit. This comparator is introduced as a necessary reference in order to deduce relative results that facilitate the interpretation in terms of emission reduction.

Scenario analysis. Fig. 4 features the GWP100 results of all 30 studied scenarios in the scenario analysis.

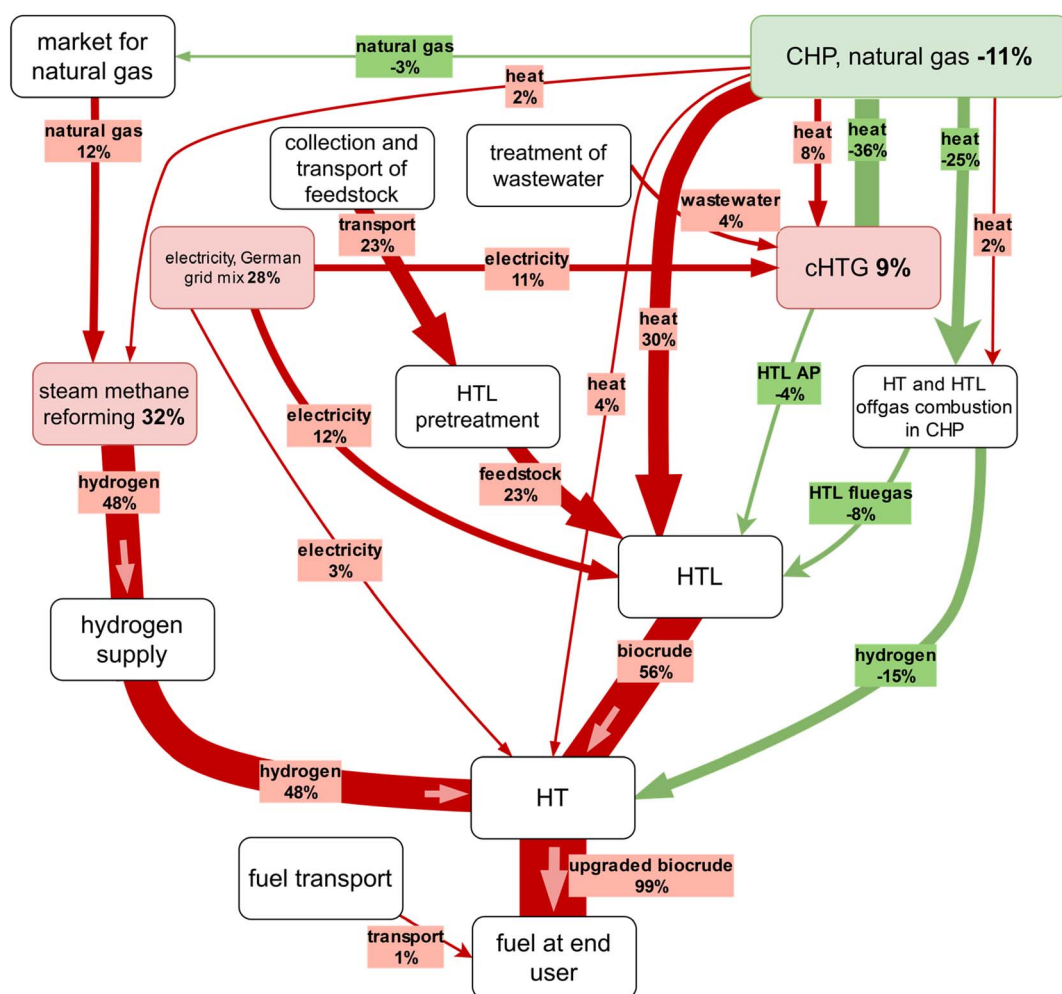


Fig. 3 LCA Sankey diagram of the baseline case BL-SMR-NG-GGM-M1. Electricity input is modelled as the grid mix of Germany with a GWP100 of 410 g CO₂-eq. kW⁻¹ h⁻¹. Major impacts can be observed from H₂ supply and heat demand. 100% is defined as the GWP100 value of the whole process. Emissions are denoted in red, while avoided emissions are shown in green. Process steps shown in white do not have direct emissions linked to the process, while process steps shown in red involve direct emissions (e.g. steam methane reforming, SMR). Each percentage gives the amount of emissions of a specific stream of process in relation to the amount of emissions of the whole fuel production process. The threshold impact is chosen as 1%.



Analysing the M1-scenarios, it can be observed that the GWP100 value of the baseline case is 1.18 kg CO₂-eq. per kg_{fuel mix}. The two alternative H₂ supply scenarios (AEL-BG-GGM-M1 and SMR-BG-GGM-M1) display emissions of 2.25 and 0.87 kg CO₂-eq. per kg_{fuel mix}, respectively. When furthermore changing the heat input from natural gas to electrical heating (AEL-EL-GGM-M1 and SMR-EL-GGM-M1), emissions are found to increase significantly. With the constraint that the electricity input was only changed in the foreground system, it becomes clear that a lower carbon intensity of the electricity input leads to lower GWP100 emissions for every process configuration.

To study the influence of the type of manure, all M1-scenarios are contrasted with their respective M2-scenarios. While the observed trends for M2-scenarios are fully consistent with what is found for the baseline feedstock M1, each M2-scenario shows a lower GWP100 value compared to its respective M1 counterpart. This can be explained by the higher organic content (lower ash content) in manure 2, leading to higher biocrude and fuel yields, thereby decreasing the impact per kg_{fuel mix} produced. For the baseline configuration, replacing the feedstock with M2 leads to an impact reduction of roughly 30% (1.18 kg CO₂-eq. per kg_{fuel mix} to 0.80 kg CO₂-eq. per kg_{fuel mix}, respectively).

Within each process configuration, differences between the corresponding M1 and M2 scenarios grow with increasing carbon intensity of the electricity input. Within each electricity input, the differences between respective M1 and M2 scenarios are highly dependent on the process configuration and the respective electricity input. All investigated scenarios show GWP100 results below the emissions of conventional jet fuel production. According to the European Renewable Energy Directive II (EU RED II), biofuels consumed in the transport sector need to show a GHG

emission saving of 65% or more compared to the fossil comparator.⁴⁵ Using an electricity mix with a high or medium share of renewable electricity as electricity input, all studied scenarios are well below this threshold. Employing the GGM from 2019 as electricity input, half of the studied scenarios do not show sufficient emission savings. RED II-compliant scenarios are BL-GGM-M1/M2, BL-NG-M1/M2, SMR-BG-GGM-M1/M2, SMR-BG-NG-M1/M2, SMR-EL-GGM-M2 and SMR-EL-NG-M2.

Out of all considered scenarios, AEL-EL-CI1-M2 shows the highest GHG emission reduction potential amounting to 98.6% (*i.e.* 0.05 kg CO₂-eq. per kg_{fuel mix}), followed by SMR-EL-CI1-M2 (95.6%) and AEL-NG-CI1-M2 (95.5%). AEL-EL-CI1-M1 presents a reduction potential of 94.2%.

Interestingly, several shifts of the best performing scenario with varying electricity input can be observed. Using the GGM from 2019 as electricity input shows that the SMR-NG-scenarios have the highest reduction potential, while an electricity input with a medium share of renewables leads to the SMR-EL-scenarios having the highest GWP100 reduction potential. An electricity input with a high share of wind favours the AEL-EL-scenarios. Based on these findings, actual transition points and regimes for the best performing scenarios with manure 1 as feedstock are investigated.

Fig. 5 depicts the GWP100 scores of M1 scenarios with the carbon intensity of the electricity source as a continuous variable. Different slopes correspond to different sensitivities of the respective process configurations to the carbon intensity of the electricity source. The BL and SMR-BG process configurations have the same electrical energy demand (2.9 MJ_{el} kg_{fuel mix}⁻¹), while heating the SMR scenarios with electrical resistance heating leads to a significant increase of electrical energy demand (SMR-EL, 12.0 MJ_{el} kg_{fuel mix}⁻¹). Using electrolysis for H₂ provision

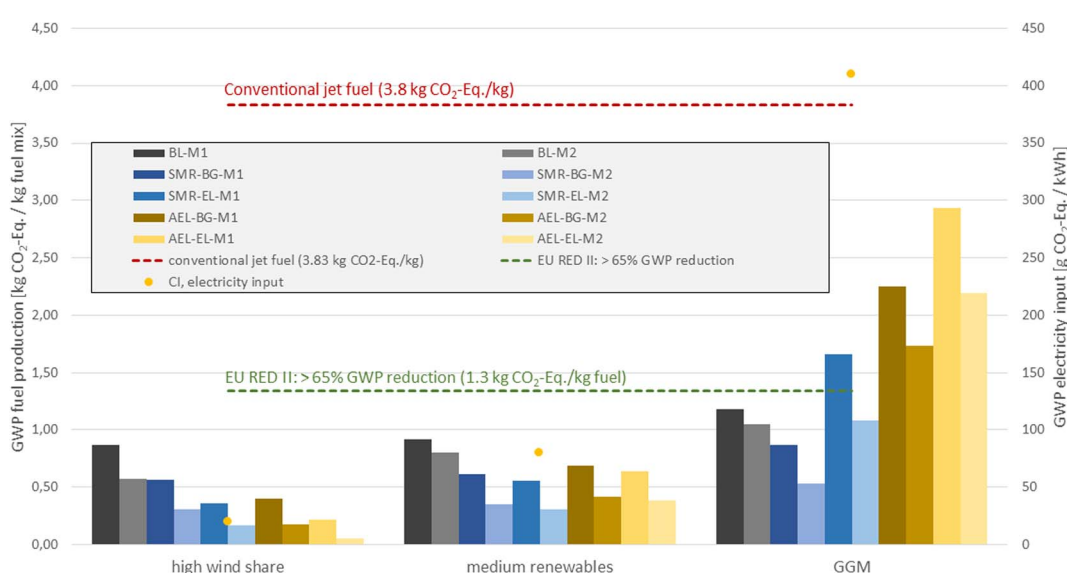


Fig. 4 GWP of HTL fuel production for scenarios BL, SMR-BG, SMR-EL, AEL-BG and AEL-EL with manure 1 and manure 2 as feedstock (from left to right). Grey bars show BL scenarios, blue bars show SMR scenarios (BG: dark, EL: bright) and yellow bars show AEL scenarios (BG: bright, EL: dark). Results for manure 1 are always shown on the left side, results for manure 2 are next to manure 1 results on the right. Yellow dots indicate the carbon intensity of the respective electricity input used. Emissions associated with conventional jet fuel production are indicated by a red dashed line (3.8 kg CO₂-eq. per kg_{fuel mix}), while the green dashed line shows the threshold of the EU RED II for biofuels (1.3 kg CO₂-eq. per kg_{fuel mix}; 65% reduction compared to fossil comparator).³⁸



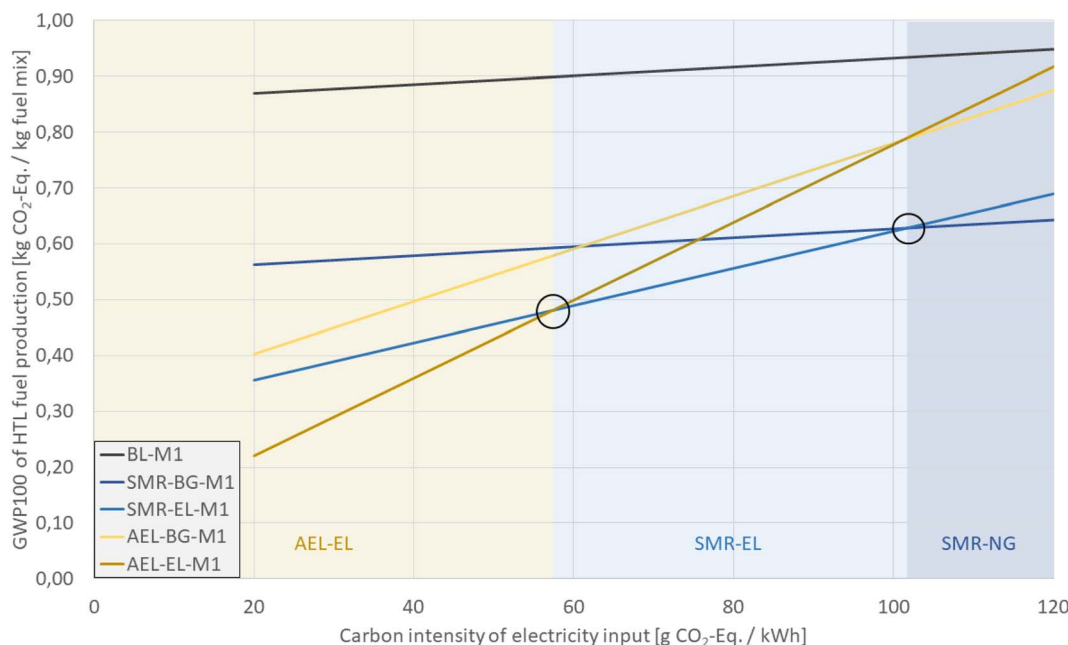


Fig. 5 Dependency of GWP100 of fuel production on emission intensity of electricity input. SMR-EL-M1, AEL-BG-M1 and AEL-EL-M1 scenarios show a strong dependency on the carbon intensity of the electricity input due to either electrical heating or H₂ supply via AEL or both. BL-M1 and SMR-BG-M1 scenarios are rather insensitive to changes in the carbon intensity of the electricity input.

further raises demand ($17.0 \text{ MJ}_{\text{el}} \text{ kg}_{\text{fuel mix}}^{-1}$). Consequently, the highest electricity input is found for the AEL-EL scenarios ($25.1 \text{ MJ}_{\text{el}} \text{ kg}_{\text{fuel mix}}^{-1}$). Electricity demands for the M2-scenarios as well as a comparison to other fuel production pathways, which also show a noticeable electricity demand can be found Table S11.†

Besides revealing the electricity demand of each process configuration, Fig. 5 also provides regimes in which different

process configurations excel. When only high carbon-intensive electricity, such as the GGM from 2019, is available at the site of production, the SMR-BG outperforms the other configurations. At an intermediate carbon intensity of around $80 \text{ g CO}_2\text{-eq. kW}^{-1} \text{ h}^{-1}$ (CI2), which may be achieved in Germany when the 2030 political targets of coal phase out and an 80% renewable electricity share is achieved, SMR-EL is found to be the favourable

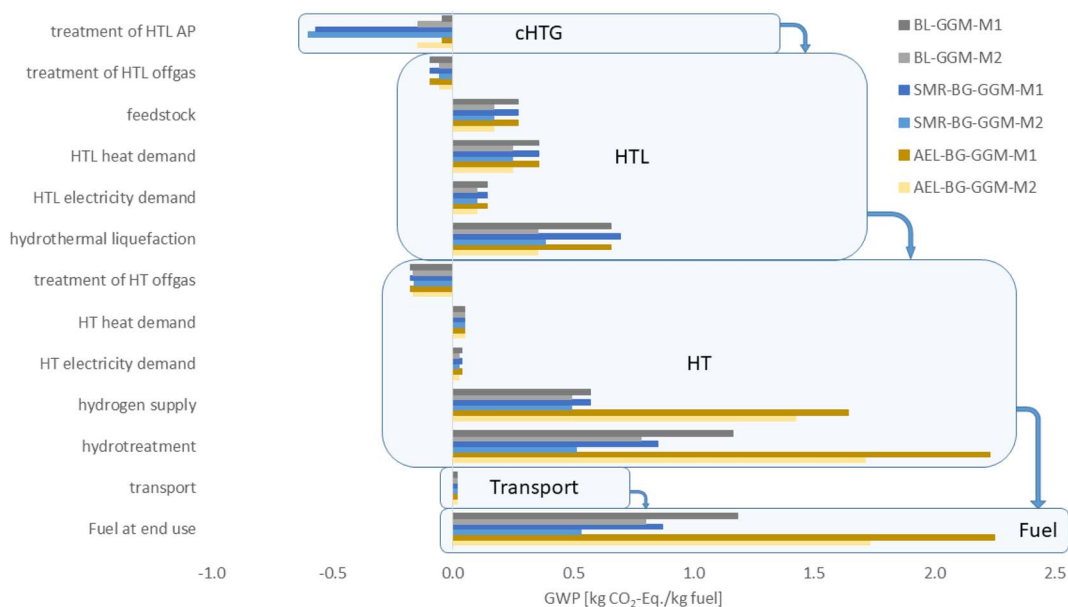


Fig. 6 GWP100 of individual process steps of the HTL fuel production process chain with GGM ($410 \text{ g CO}_2\text{-eq. kW}^{-1} \text{ h}^{-1}$) as electricity technology. Scenarios BL-M1, BL-M2, SMR-BG-M1, SMR-BG-M2, AEL-BG-M1 and AEL-BG-M2 are shown. Dark grey bars: BL-M1, light grey bars: BL-M2, dark blue bars: SMR-M1, light blue bars: SMR-M2, dark yellow bars: AEL-BG-M1, light yellow bars: AEL-BG-M2.



Table 5 Heat balance for scenarios BL-M1, BL-M2, SMR-M1, SMR-M2, AEL-M1 and AEL-M2 normalized to the production of 1 kg of HTL fuel mix. All values are given in MJ/kg_{fuel mix}

	process step	BL-M1	BL-M2	SMR-M1	SMR-M2	AEL-M1	AEL-M2
Demands	H ₂ separator (SMR)	0.03	0.03	0.03	0.03	0	0
	HTL	12.5	8.7	12.5	8.7	12.5	8.7
	HT	1.8	1.8	1.8	1.8	1.8	1.8
	SMR	1.0	0.9	1.0	0.9	0.0	0.0
	Treatment of HT offgas <i>via</i> PSA	0.6	0.4	0.6	0.4	0.6	0.4
	Treatment of HTL AP retentate	3.3	2.5	3.3	2.5	3.3	2.5
Sum		19.3	14.3	19.3	14.3	18.2	13.4
Production	Fluegas from HTL	3.4	1.9	3.4	1.9	3.4	1.9
	Fluegas from HT	6.8	6.2	6.8	6.2	6.8	6.2
Sum Difference		10.2	8.1	10.2	8.1	10.2	8.1
Use of biogas	Remaining heat demand	9.1	6.2	9.1	6.2	8.0	5.3
	Biogas production	15.0	15.6	15.0	15.6	15.0	15.6
	Biogas for SMR	0	0	7.8	6.8	0	0
	Biogas to custom market for heat	0	0	7.2	6.2	8.0	5.3
Use of external natural gas	Biogas to custom market for heat – substitution	15.0	15.6	0	2.6	7.0	10.3
	External NG demand	9.1	6.2	1.9	0	0	0

process configuration. Low CIs of around 20 g CO₂-eq. kW⁻¹ h⁻¹ may *e.g.* correspond to a renewable electricity mix with a high share of wind electricity. In this case, AEL-EL-scenarios result in significant emission savings. From the results, it can be concluded that producing H₂ *via* AEL for the use in the HTL fuel production pathway is only recommended when using an electricity mix with a high share of renewables. As indicated in Fig. 5, exact transition points are at 57.4 g CO₂-eq. kW⁻¹ h⁻¹ and 101.6 g CO₂-eq. kW⁻¹ h⁻¹, however, these are only viable for the herein discussed process configurations. Instead of fixed values, we rather want to emphasize the general trend of the different regimes and best performing process configurations.

Relevance of internal biogas production. Fig. 6 breaks down the emission sources for the BL scenario and both SMR-BG and AEL-BG alternatives, whereat both manure samples are considered and GGM (410 g CO₂-eq. kW⁻¹ h⁻¹) is used as the electricity input. Notably the most pronounced differences among process configurations are observed in the activities “treatment of HTL AP” and “H₂ supply”. These observations are tied to internal biogas production – a central aspect of the assessment presented herein as it couples aqueous phase treatment, H₂ supply and heat supply and therefore determines the need for external natural gas. In the following, we aim to detangle these interrelations for each process configuration:

- BL scenarios: heat demand and H₂ production are covered solely by externally purchased natural gas.

- The CH₄ required to produce H₂ leads to a fixed amount of emissions for H₂ supply.

- SMR-M1 scenario: internally produced biogas can feed H₂ production and partially cover heat demand. Ca. 10% of the total heat demand has to be met by external natural gas (see Table 5). Compared to the baseline scenario, emissions are saved by replacing fossil H₂ production.

- SMR-M2 scenario: Internally produced biogas is sufficient to cover heat demand and H₂ production; excess biogas is used to substitute heat on the market.

- AEL scenarios: No biogas is required for H₂ production. Internally produced biogas covers the heat demand, which is slightly lower due to the removed SMR unit. Internally produced surplus biogas substitutes heat on the market.

Moreover, two major insights on the choice of manure are obtained. First, heat demand of M2 scenarios is around 26% lower compared to M1 scenarios as less feedstock is used and therefore less slurry needs to be heated. This effect is caused by the favourable chemical composition of M2. Secondly, the amount of produced biogas is independent of the process configuration and shows only a minor dependence on the manure sample.

LCA of HTL fuel production pathway – consequential approach

In the following sections, the results of the consequential approach will be presented.

Emission savings from manure storage. Table 6 lists three scenarios for GHG emissions from manure storage in Germany. The minimum (MIN) scenario would entail storing all manure in solid storage, while the maximum (MAX) scenario corresponds to storage in uncovered anaerobic lagoons. Additionally, an estimated average emission value was derived from the FAOSTAT database.¹⁰⁻¹² Details on the calculations can be found

Table 6 MIN (solid storage) and MAX (storage: uncovered anaerobic lagoons) GHG emissions for manure storage in Germany based on ref. 10 and estimated value derived from ref. 10–12. All values are given in kg CO₂-eq. per kg manure

Scenario	GWP100 [kg CO ₂ -eq. per kg manure]
MIN	0.36
MAX	3.71
Estimated value	0.60



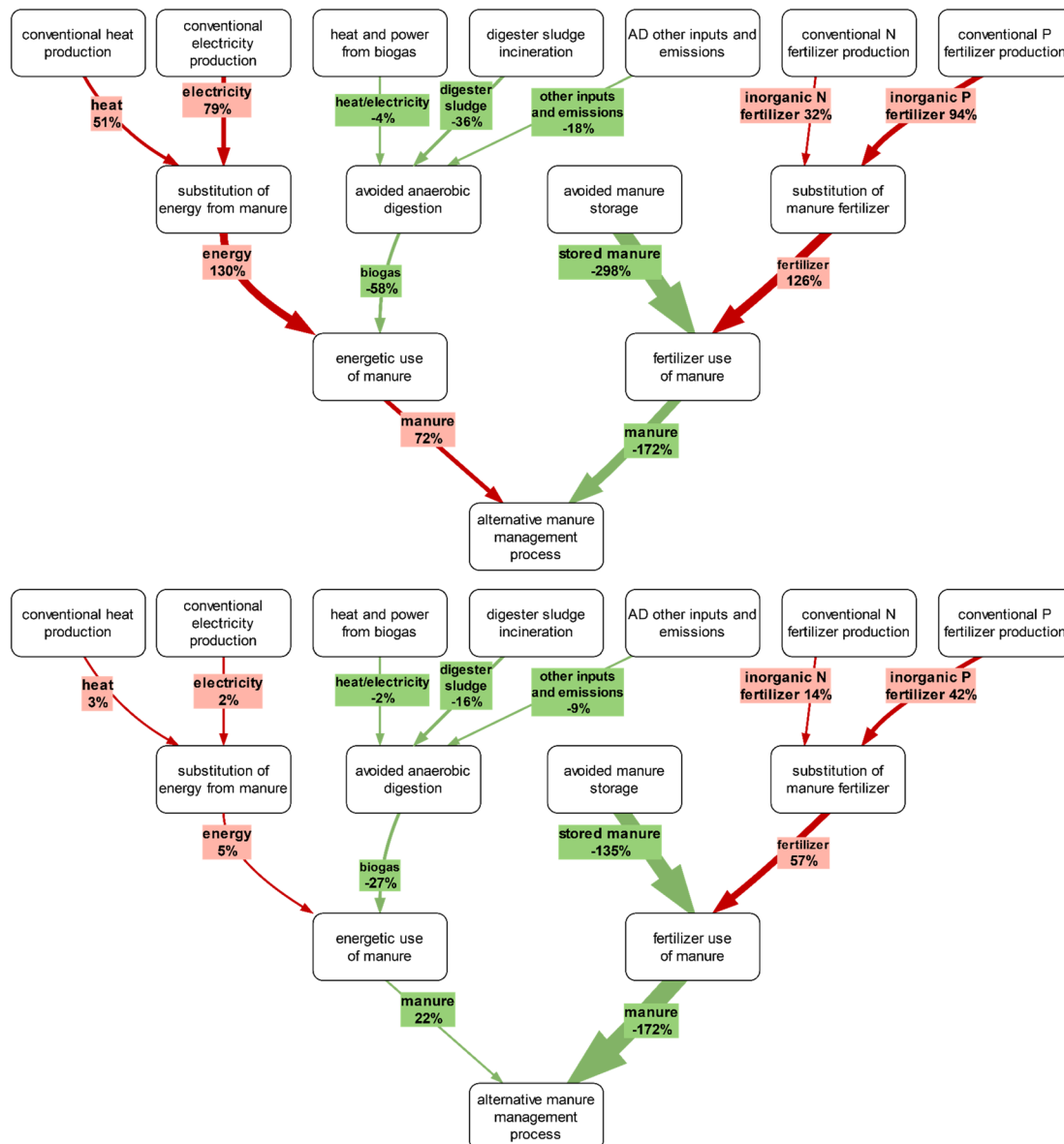


Fig. 7 Sankey diagram of the manure reference process. (A) BL-scenario, (B) scenario with CI1 as electricity input and EL for heating. -100% is defined as the GWP100 value of the manure reference process. Emissions are denoted in red, while avoided emissions are shown in green. Process steps shown in white do not have direct emissions linked to the process, while process steps shown in red involve direct emissions (e.g. manure storage emission savings). Each percentage gives the amount of emissions of a specific stream of process in relation to the amount of emissions of the whole fuel production process.

in the SI. It is important to note that the listed values are the result of manure storage over several months, which is the case as manure is stored since its targeted use as a fertilizer is bound to seasonal growth periods. For HTL conversion it is assumed that the storage duration is reduced to 14 days. The modelling results suggest that around 93% of the emissions related to manure storage can be saved due to the shorter storage duration.

Emissions savings from alternative manure management. Based on these findings we investigate the emission saving potential of an alternative manure management process with reduced storage time of manure before usage.

Overall, manure-assigned emissions are a combination of emission savings from shortened manure storage, emissions attributed to foregone benefits and emissions savings by avoided burdens. Fig. 7A shows the Sankey diagram of the alternative manure management process based on the estimated emission value from the FAOSTAT database and the input parameters from the baseline case of the cut-off approach (namely: CI of GGM: 410 g CO₂-eq. kW⁻¹ h⁻¹ and heat from natural gas). Emissions are clearly dominated by emission savings from manure storage (-298%). Other avoided burdens arise from the avoidance of emissions related to the anaerobic digestion of manure. However, foregone benefits also show a significant impact. Fertilizer use of manure (-126%) as well as



energetic use of manure (72%) both play a major role. In the case of fertilizer use, manure has to be substituted by inorganic fertilizer. In the case of energetic use of manure, foregone heat and electricity are produced *via* NG and the GGM, leading to significant amounts of emissions. However, due to the large amount of saved emissions attributed to shorter manure

storage, the overall alternative manure management process still has a negative impact ($-0.12 \text{ kg CO}_2\text{-Eq. per kg manure}$).

Fig. 7B shows the Sankey diagram of the alternative manure management process with CI1 as electricity input and electrical heating. In comparison to the BL alternative manure management process, a significant difference for the foregone benefit of

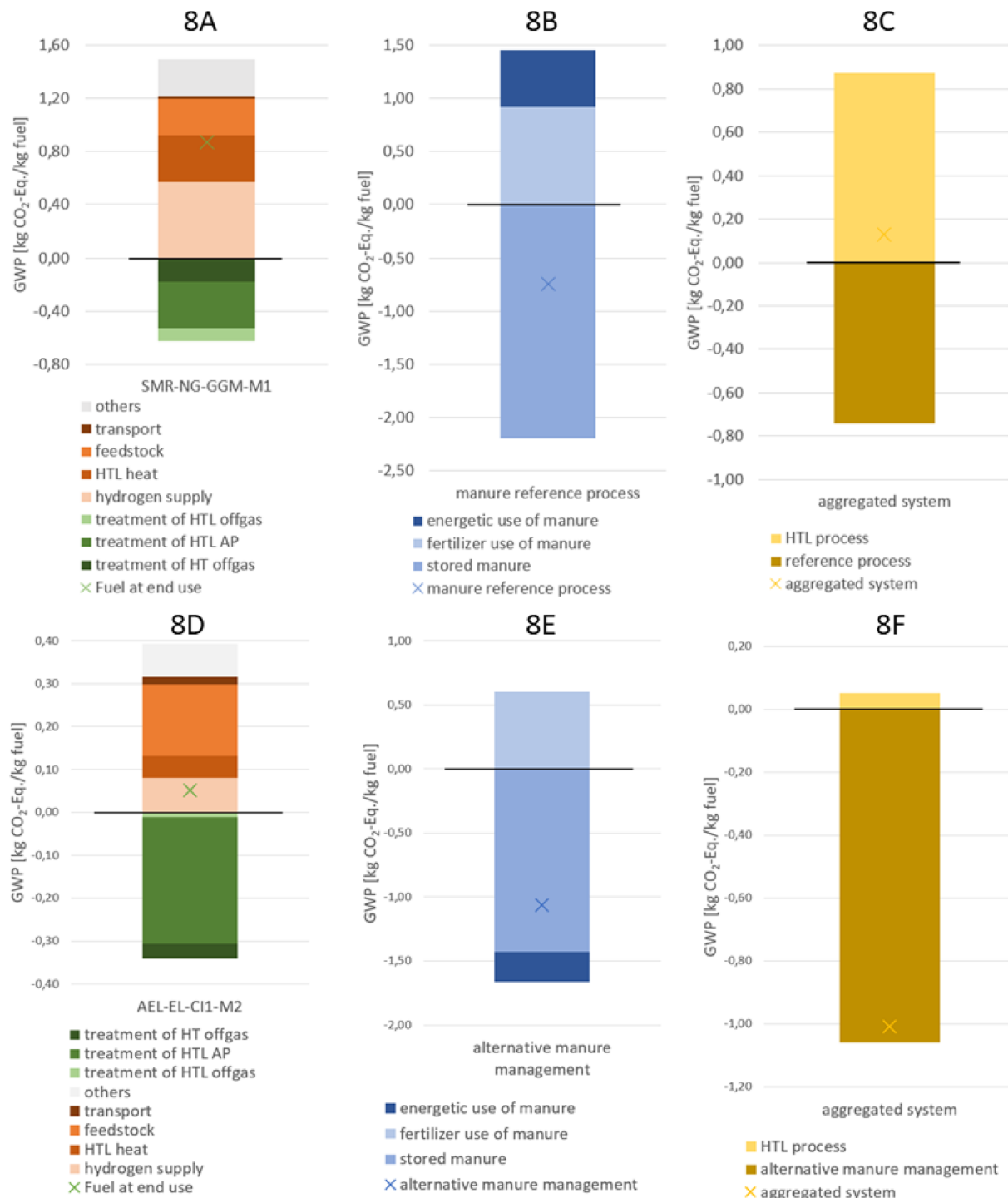


Fig. 8 GWP100 results depicted as stacked bar charts: (a) scenario SMR-BG-GGM-M1. (b) Alternative manure management process for scenario SMR-BG-GGM-M1. (c) Aggregation of scenario SMR-BG-GGM-M1 and the respective alternative manure management. (d) Scenario AEL-EL-PV-M2. (e) Alternative manure management process for scenario AEL-EL-PV-M2. (f) Aggregation of scenario AEL-EL-PV-M2 and the respective alternative manure management process.



substitution of energy from manure can be observed. This can be explained by the very low GWP of the electricity and heat production, considering CI1 as input. In fact, producing heat and electricity from manure becomes less attractive when electricity can be produced with such a low CI. This is indicated by emission savings of 22% compared to the foregone benefit of 72% in the BL case. The proportions of results for the fertilizer use of manure are identical to the BL case. Having said this, the overall impact of the CI-EL manure management scenario is more negative compared to the BL scenario ($-0.28 \text{ kg CO}_2\text{-eq. per kg manure}$), which means that using manure for HTL is overall beneficial from a GWP perspective.

Consequential approach compared for different process configurations

Assuming the use of manure M1 in Germany in 2019, scenario SMR-NG-GGM-M1 shows the lowest GWP100 ($0.87 \text{ kg CO}_2\text{-eq. per kg}_{\text{fuel mix}}$) in the cut-off approach, whereby the individual contributions are highlighted in Fig. 8A. In Fig. 8B, the impact of the alternative manure management process becomes evident: said scenario amounts to emission savings of $-0.74 \text{ kg CO}_2\text{-eq. per kg}_{\text{fuel mix}}$. The overall impact of the emission savings assigned to manure is illustrated in Fig. 8C: the result of the consequential approach reveals a significantly reduction of the GWP100 ($0.13 \text{ kg CO}_2\text{-eq. per kg}_{\text{fuel mix}}$).

In order to further demonstrate the effect of an alternative manure management, we replicate the assessment for a different scenario, namely the electrolysis-based AEL-EL-CI1-M2 which also includes a different manure management scenario. As expected, the emission profile for the cut-off approach differs quite significantly (Fig. 8D) from the SMR-based process discussed above. A smaller manure requirement when using M2 would suggest lower emission savings for CI1-EL, however, due to the lower CI of the electricity market and electrical heating, the emission savings of the alternative manure management (Fig. 8E) are increased by *ca.* 43% compared to the BL scenario. Overall, this results in negative emissions of $-1.01 \text{ kg CO}_2\text{-eq. per kg}_{\text{fuel mix}}$ (Fig. 8F) and – once again – manure management accounts for the largest part of the savings, confirming the hypothesis that there is a huge emission saving potential when reducing the manure storage time.

Model limitations and future work

This work represents a LCA of HTL in various process configurations. While the analysis has been conducted thoroughly and to the best of our abilities, data availability limits accuracy at certain points, especially where assumptions had to be implemented in the LCI phase:

- Wastewater streams appear in the cHTG process step and in the nutrient recovery. Experimentally it could be proven that the wastewater of the cHTG process step does not contain large amounts of contaminants, while it is qualitatively understood that wastewaters, *e.g.* from nutrient recovery, are significantly more polluted. Quantitative analysis have not been performed

and no inventory data is available for the wastewaters of HTL processes.

- Fertilizer products appear as manure itself, the digestate of anaerobic digestion of manure, struvite in the nutrient recovery process and conventional inorganic fertilizer. Depending on their bioavailability, these different fertilizer products are associated with varying potency. Again, no quantitative data on these influences are available and model accuracy will benefit from future research.

- Another inaccuracy is generated by the dependence of the fuel mix resulting from HTL on manure composition. In this work, two different manure compositions have been analyzed. This analysis could be further extended to include a broad range of compositions, in order to well-represent the large variety observed in manure samples.

- Within this analysis, it was assumed that the organic content of the HTL process water is treated and utilized by cHTG. Alternative treatment strategies may be implemented in the future.

- Furthermore, modelling an overarching heat recovery network for the process would allow a more careful investigation of the impact of that parameter.

- The quantitative assessment of the manure management process could further be improved by more in-depth data acquisition on country-specific manure volumes and compositions and a more detailed model of the temperature dependence of manure storage.

Finally, regarding the LCIA phase, it should be noted that extending this assessment to other impact categories beyond GWP100 would yield valuable insights. In particular, it is known that current manure handling practices can lead to significant water^{46,47} and air⁴⁸ quality issues. This was, however, beyond the scope of this manuscript that focusses on GWP.

Future work should include closing the gaps of missing data as well as the investigation of alternative treatment and valorization options for the HTL AP. These could *e.g.* include aqueous phase reforming of the HTL AP for *in situ* H₂ production or wet oxidation of the HTL AP for process heat generation.^{49,50}

An important aspect of future work is the evaluation of the investigated process configurations with respect to economic performance parameters. Investigations of a coupling of advanced biomass conversion with renewable hydrogen generation revealed that both biogenic feedstock cost and electricity cost are key for an economically competitive fuel production. Both parameters are highly variable. Manure is a valuable fertilizer in some regions, while it poses a disposal problem in regions with high livestock density. Electricity costs are highly dependent on local wind and solar resources and can significantly depend on country specific regulations, especially when grid electricity is used.

Conclusions

In this paper, LCAs of different HTL fuel production process configurations in Germany have been performed. In the



baseline case (BL) heat and H₂ is produced from natural gas, the latter *via* SMR. Manure is considered as the feedstock with a cut-off approach. The GWP100 for the baseline case was determined as 1.18 kg CO₂-eq. per kg_{fuel mix}, which shows significant reduction potential compared to conventional jet fuel production (3.83 kg CO₂-eq. per kg_{fuel mix}). Heat production for the HTL reaction, as well as H₂ production for the subsequent hydro-treatment were identified as the main emission drivers (Fig. 3). To investigate potential alternative solutions to the main emission drivers, H₂ provision from AEL and process heat generation from electricity was studied.

While all scenarios perform better than conventional jet fuel, this is not true for the EU RED II threshold. AEL scenarios, as well as the scenario SMR-EL-M1, all run with the GGM as electricity input show higher emissions than 1.3 kg CO₂-eq. per kg_{fuel mix}. Furthermore, it was observed that within one manure sample, three different process configurations performed best with varying electricity input. Electricity inputs with a high CI favour the SMR-NG scenario, while medium CIs favour the introduction of electrical heating (SMR-EL scenario) and low CIs suggest the introduction of both electrical heating and alkaline electrolysis for H₂ production (AEL-EL scenario). It can be concluded that electrolysis for H₂ production and electrical heating to a minor extent present interesting options to reduce emissions when using green electricity.

Manure M2 scenarios show a better performance compared to manure M1 scenarios, due to the lower ash content of manure M2. In consequence, the organic fraction is larger, leading to a smaller amount of feedstock input and subsequently lower GWP100 emissions.

Finally, a consequential LCA approach was introduced. Current manure management is accompanied with high amounts of GHG emissions, mostly stemming from manure storage. The amount of emissions is highly dependent on the temperature and the duration of storage. It is proposed that HTL can lead to significant reductions in GWP100 of manure management due to shorter storage times. Compared to current manure management practice, the herein used manure reference model suggests that -0.38 kg CO₂-eq. per kg manure can be saved when using HTL. This leads to HTL with manure as feedstock being a carbon negative fuel production pathway in most consequential scenarios. However, it should be mentioned that emission savings are generated independent on the technology used, as long as the storage duration is reduced significantly.

Author contributions

Conceptualization: L. M., B. P., C. P. K. E. and V. B.; methodology, L. M., B. P.; validation, L. M., B. P. and V. B.; formal analysis, L. M. and B. P.; investigation, L. M. and B. P.; writing—original draft preparation, L. M.; writing—review and editing, L. M., B. P., V. B., K. E. and C. P.; visualization, L. M.; supervision, K. E. and V. B.; project administration, V. B. All authors have read and agreed to the published version of the manuscript.

Conflicts of interest

There are no conflicts to declare.

Acknowledgements

This project has received funding from the European Union's Horizon 2020 research and innovation programme under grant agreement No. 764734. The present studies have been carried out in the project GNOSIS, funded by the German national research funding LuFo VI (Luftfahrtforschungsprogramm). The authors would like to acknowledge the support of Germany's Federal Ministry for Economic Affairs and Climate Action (BMWK).

Notes and references

- 1 UNFCCC, *Paris Agreement*, United Nations, Geneva, 2015, https://unfccc.int/sites/default/files/english_paris_agreement.pdf.
- 2 Umweltbundesamt, *Emissionsquellen in Deutschland*, <https://www.umweltbundesamt.de/themen/klima-energie/treibhausgas-emissionen/emissionsquellen#energie-stationar>, accessed 24 April 2023.
- 3 Umweltbundesamt, *Beitrag der Landwirtschaft zu den Treibhausgas-Emissionen*, <https://www.umweltbundesamt.de/daten/land-forstwirtschaft/beitrag-der-landwirtschaft-zu-den-treibhausgas-emissionen-aus-der-landwirtschaft>, accessed 24 April 2023.
- 4 European Environment Agency, *EEA Greenhouse Gases - Data Viewer*, <https://www.eea.europa.eu/data-and-maps/data/data-viewers/greenhouse-gases-viewer>, accessed 24 April 2023.
- 5 The International Council on Clean Transportation, *Transport Could Burn up the EU's Entire Carbon Budget*, <https://theicct.org/transport-could-burn-up-the-eus-entire-carbon-budget/>, accessed 24 April 2023.
- 6 V. Batteiger, K. Ebner, H. Antoine, L. Moser, P. Schmidt, W. Weindorf and T. Raksha, *Power-to-Liquids - A Scalable and Sustainable Fuel Supply Perspective for Aviation, Background*, Dessau-Roßlau, 2022, <https://www.umweltbundesamt.de/publikationen/power-to-liquids>.
- 7 Praxis-Agrar - BLE: *Wie viel Wirtschaftsdünger wird auf deutschen Äckern und Grünland ausgebracht?*, <https://www.praxis-agrar.de/pflanze/ackerbau/duengung/wieviele-wirtschaftsduenger-wird-auf-aeckern-und-gruenland-ausgebracht>, accessed 24 April 2023.
- 8 S. Bundesamt, *Landwirtschaftliche Betriebe und Menge an Wirtschaftsdünger auf Ackerland oder Dauergrünland ausgebracht haben, nach Düngerarten*, <https://www.destatis.de/DE/Themen/Branchen-Unternehmen/Landwirtschaft-Forstwirtschaft-Fischerei/Produktionsmethoden/Tabellen/landwirtschaftliche-betriebe-wirtschaftsduenger.html?nn=371820>, accessed 24 April 2023.



9 P. Mielcarek-Bocheńska and W. Rzeźnik, Greenhouse Gas Emissions from Agriculture in EU Countries—State and Perspectives, *Atmosphere*, 2021, **12**, 1396.

10 O. Gavrilova, A. Leip, H. Dong, J. D. Macdonald and T. V. Vellinga, in *2019 Refinement to the 2006 IPCC Guidelines for National Greenhouse Gas Inventories*, ed. Z. Zhu, et al., 2019.

11 FAOSTAT, *Emissions from Manure Management*, <https://www.fao.org/faostat/en/#data/GT>, accessed 24 April 2023.

12 FAOSTAT, *Livestock Data for European Countries*, <https://www.fao.org/faostat/en/#data/GT>, accessed 24 April 2023.

13 M. S. Haider, D. Castello and L. A. Rosendahl, Two-stage catalytic hydrotreatment of highly nitrogenous biocrude from continuous hydrothermal liquefaction: a rational design of the stabilization stage, *Biomass Bioenergy*, 2020, **139**, 105658.

14 S. Yin, R. Dolan, M. Harris and Z. Tan, Subcritical hydrothermal liquefaction of cattle manure to bio-oil: effects of conversion parameters on bio-oil yield and characterization of bio-oil, *Bioresour. Technol.*, 2010, **101**, 3657–3664.

15 J. S. dos Passos, A. Matayeva and P. Biller, Synergies during hydrothermal liquefaction of cow manure and wheat straw, *J. Environ. Chem. Eng.*, 2022, **10**, 108181.

16 D. R. Vardon, B. K. Sharma, J. Scott, G. Yu, Z. Wang, L. Schideman, Y. Zhang and T. J. Strathmann, Chemical properties of biocrude oil from the hydrothermal liquefaction of Spirulina algae, swine manure, and digested anaerobic sludge, *Bioresour. Technol.*, 2011, **102**, 8295–8303.

17 J. Lu, J. Watson, J. Zeng, H. Li, Z. Zhu, M. Wang, Y. Zhang and Z. Liu, Biocrude production and heavy metal migration during hydrothermal liquefaction of swine manure, *Process Saf. Environ. Prot.*, 2018, **115**, 108–115.

18 C. S. Theegala and J. S. Midgett, Hydrothermal liquefaction of separated dairy manure for production of bio-oils with simultaneous waste treatment, *Bioresour. Technol.*, 2012, **107**, 456–463.

19 H. Li, J. Lu, Y. Zhang and Z. Liu, Hydrothermal liquefaction of typical livestock manures in China: biocrude oil production and migration of heavy metals, *J. Anal. Appl. Pyrolysis*, 2018, **135**, 133–140.

20 J. Lu, H. Li, Y. Zhang and Z. Liu, *Nitrogen Migration and Transformation during Hydrothermal Liquefaction of Livestock Manures*, ACS Sustainable Chemistry & Engineering, 2018.

21 T. Horschig, C. Penke, A. Habersetzer and V. Batteiger, *Public Report - Report on Feedstock Potentials and Preference Regions for HTL Projects*, 2019, https://www.bauhaus-luftfahrt.net/fileadmin/user_upload/Publikationen/Horschig_D1-3_HTL_preference_regions.pdf, accessed 19 July 2023.

22 DIN EN ISO 14040:2021-02, Umweltmanagement-Ökobilanz-Grundsätze und Rahmenbedingungen (ISO14040:2006+Amd1:2020); Deutsche Fassung EN ISO 14040:2006+A1:2020, Beuth Verlag GmbH, Berlin.

23 DIN EN ISO 14044:2018-05, Umweltmanagement-Ökobilanz-Anforderungen und Anleitungen (ISO_14044:2006+Amd_1:2017); Deutsche Fassung EN ISO 14044:2006+A1:2018, Beuth Verlag GmbH, Berlin.

24 C. Mutel, Brightway: an open source framework for Life Cycle Assessment, *J. Open Source Softw.*, 2017, **2**, 236.

25 G. Wernet, C. Bauer, B. Steubing, J. Reinhard, E. Moreno-Ruiz and B. Weidema, The ecoinvent database version 3 (part I): overview and methodology, *Int. J. Life Cycle Assess.*, 2016, **21**, 1218–1230.

26 M. A. J. Huijbregts, Z. J. N. Steinmann, P. M. F. Elshout, G. Stam, F. Verones, M. Vieira, M. Zijp, A. Hollander and R. van Zelm, ReCiPe2016: a harmonised life cycle impact assessment method at midpoint and endpoint level, *Int. J. Life Cycle Assess.*, 2017, **22**, 138–147.

27 D. S. Schimel, D. Alves, I. G. Enting, M. Heimann, F. Joos, D. Raynaud, T. M. L. Wigley, M. J. Prather, R. Derwent, D. Ehhalt, P. J. Fraser, E. Sanhueza, X. Zhou, P. Jonas, R. Charlson, H. Rodhe, S. Sadasivan, K. P. Shine, Y. Fouquet, V. Ramaswamy, S. Solomon, Srinivasan, D. L. Albritton, I. Isaksen, M. Lal and D. Wuebbles, *Radiative Forcing of Climate Change*, Cambridge University Press, Cambridge, 1996.

28 G. Myhre, D. Shindell and J. Pongratz, *Anthropogenic and Natural Radiative Forcing*, Cambridge University Press; Ludwig-Maximilians-Universität München, Cambridge, 2014.

29 L. Moser, C. Penke and V. Batteiger, *An In-Depth Process Model for Fuel Production via Hydrothermal Liquefaction and Catalytic Hydrotreating Processes*, 2021, pp. 1172–1179.

30 HyFlexFuel Project, <https://www.hyflexfuel.eu/>, accessed 24 April 2023.

31 C. Penke, L. Moser and V. Batteiger, Modeling of cost optimized process integration of HTL fuel production, *Biomass Bioenergy*, 2021, **151**, 106123.

32 Eurostat, *Glossary: manure*, <https://ec.europa.eu/eurostat/statistics-explained/index.php?title=Glossary:Manure&oldid=476892>, accessed 24 April 2023.

33 P. L. Spath and M. K. Mann, *Life Cycle Assessment of Hydrogen Production via Natural Gas Steam Reforming*, National Renewable Energy Lab. (NREL), Golden, CO (United States), NREL/TP-570-27637, <https://www.osti.gov/biblio/764485>.

34 N. Scarlat, M. Prussi and M. Padella, Quantification of the carbon intensity of electricity produced and used in Europe, *Appl. Energy*, 2022, **305**, 117901.

35 Communication from the Commission to the European Parliament, the Council, the European Economic and Social Committee and the Committee of the Regions, <https://www.eea.europa.eu/policy-documents/communication-from-the-commission-to-1>, accessed 24 April 2023.

36 E. Taibi, H. Blanco, R. Miranda and M. Carmo, *Green Hydrogen Cost Reduction: Scaling up Electrolyzers to Meet the 1.5°C Climate Goal*, The International Renewable Energy Agency (IRENA), Abu Dhabi, 2020.

37 J. C. Koj, C. Wulf, A. Schreiber and P. Zapp, Site-Dependent Environmental Impacts of Industrial Hydrogen Production by Alkaline Water Electrolysis, *Energies*, 2017, **10**, 860.



38 J. Lu, H. Li, Y. Zhang and Z. Liu, *Nitrogen Migration and Transformation during Hydrothermal Liquefaction of Livestock Manures*, ACS Sustainable Chemistry & Engineering.

39 UNECE, *Life Cycle Assessment of Electricity Generation Options*, <https://unece.org/sed/documents/2021/10/reports/life-cycle-assessment-electricity-generation-options>, accessed 24 April 2023.

40 A. Müller, L. Friedrich, C. Reichel, S. Herceg, M. Mittag and D. H. Neuhaus, A comparative life cycle assessment of silicon PV modules: Impact of module design, manufacturing location and inventory, *Sol. Energy Mater. Sol. Cells*, 2021, **230**, 111277.

41 A. Cárdenas, C. Ammon, B. Schumacher, W. Stinner, C. Herrmann, M. Schneider, S. Weinrich, P. Fischer, T. Amon and B. Amon, Methane emissions from the storage of liquid dairy manure: Influences of season, temperature and storage duration, *Waste Manag.*, 2021, **121**, 393–402.

42 R. E. Thorman, D. R. Chadwick, R. Harrison, L. O. Boyles and R. Matthews, The effect on N₂O emissions of storage conditions and rapid incorporation of pig and cattle farmyard manure into tillage land, *Biosyst. Eng.*, 2007, **97**, 501–511.

43 D. Chadwick, Emissions of ammonia, nitrous oxide and methane from cattle manure heaps: effect of compaction and covering, *Atmos. Environ.*, 2005, **39**, 787–799.

44 S. Pfenniger and I. Staffell, *Weather Data*, 2020.

45 *Renewable Energy Directive II*, CELEX_32018L2001, 2022.

46 J. B. Holm-Nielsen, T. Al Seadi and P. Oleskowicz-Popiel, The future of anaerobic digestion and biogas utilization, *Bioresour. Technol.*, 2009, **100**, 5478–5484.

47 H. Steinfeld, P. Gerber, T. D. Wassenaar, V. Castel, M. Rosales and C. de Haan, *Livestock's Long Shadow. Environmental Issues and Options*, Food and Agriculture Organization of the United Nations, Rome, 2006.

48 J. Lelieveld, J. S. Evans, M. Fnais, D. Giannadaki and A. Pozzer, The contribution of outdoor air pollution sources to premature mortality on a global scale, *Nature*, 2015, **525**, 367–371.

49 G. Zoppi, E. Tito, I. Bianco, G. Pipitone, R. Pirone and S. Bensaid, Life cycle assessment of the biofuel production from lignocellulosic biomass in a hydrothermal liquefaction – aqueous phase reforming integrated biorefinery, *Renewable Energy*, 2023, **206**, 375–385.

50 L. B. Silva Thomsen, K. Anastasakis and P. Biller, Wet oxidation of aqueous phase from hydrothermal liquefaction of sewage sludge, *Water Res.*, 2022, **209**, 117863.